

# Glycyrrhizic Acid-Loaded Poly- $\epsilon$ -Caprolactone Nanoparticles Decrease PRRSV Infection in MARC-145 Cells

Samantha Jardon<sup>1</sup> , Oscar Escalona<sup>2</sup> , Carlos Gerardo García<sup>1</sup> , David Quintanar<sup>2</sup> ,  
Carlos Ignacio Soto<sup>1</sup>, María Zaida Urbán<sup>3</sup> , Susana Elisa Mendoza<sup>4\*</sup> 

<sup>1</sup>Multidisciplinary Research Unit I4 (Veterinary Morphology and Cell Biology), UNAM-FESC, Campus 4, Cuautitlán Izcalli, Mexico

<sup>2</sup>Pharmaceutical Technology Research Laboratory, UNAM-FESC, Campus 1, Cuautitlán Izcalli, Mexico

<sup>3</sup>Dr. Hideyo Noguchi Regional Research Center, UAY, Mérida, Mexico

<sup>4</sup>Laboratory of Virology and Microbiology of Respiratory Diseases of The Pig, UNAM-FESC, Campus 1, Cuautitlán Izcalli, Mexico  
Email: doctora.jardon@cuautitlan.unam.mx, \*seme@unam.mx

**How to cite this paper:** Jardon, S., Escalona, O., García, C.G., Quintanar, D., Soto, C.I., Urbán, M.Z. and Mendoza, S.E. (2023) Glycyrrhizic Acid-Loaded Poly- $\epsilon$ -Caprolactone Nanoparticles Decrease PRRSV Infection in MARC-145 Cells. *Open Journal of Veterinary Medicine*, 13, 221-236.  
<https://doi.org/10.4236/ojvm.2023.1312018>

**Received:** October 21, 2023

**Accepted:** December 5, 2023

**Published:** December 8, 2023

Copyright © 2023 by author(s) and Scientific Research Publishing Inc.

This work is licensed under the Creative Commons Attribution International License (CC BY 4.0).

<http://creativecommons.org/licenses/by/4.0/>



Open Access

## Abstract

Porcine reproductive and respiratory syndrome (PRRS) is an economically devastating disease with worldwide distribution caused by *Betaarterivirus suid* (PRRSV). The virion has great genetic and antigenic variability with a marked increase in virulence. Vaccines tested to date have been of little use in controlling the problems caused by PRRSV, so the present study was conceived to evaluate the antiviral effect of polymeric nanoparticles (PNPs) made with glycyrrhizic acid (GA). Recent work has proven that this nanoparticle system is stable. These nanoparticles have good GA carrying capacity, a size < 250 nm, a spherical morphology, and a wide safety range. The integrity of cell morphology can be maintained for up to 72 h. The antiviral effect of this nanoparticle system was tested in cultures of MARC-145 cells in pre- and coinfection assays with PRRSV to evaluate changes in cell morphology and effects on cell viability. The use of PNP<sub>s</sub>GA with the real-time quantitative polymerase chain reaction (RT-qPCR) decreased viral infection by 38% in 3 amplification cycles. These results suggest that this system has an antiviral effect against PRRSV under the study conditions established.

## Keywords

Cytotoxicity, Glycyrrhizic Acid, Cell Morphology, Polymeric Nanoparticles, PRRS Virus

## 1. Introduction

Porcine reproductive and respiratory syndrome (PRRS) is a viral disease that af-

fects domestic pigs of all ages, causing significant economic losses in the swine industry due to its devastating effect on production [1] [2]. The causative agent *Betaarterivirus suid* (PRRSV) shows great genetic and antigenic variability with a marked increase in virulence, so vaccines should be useful in controlling the problems caused [3] [4] [5].

The study of new strategies to combat this disease is a promising field of research highlighted by the development of technologies that combine the advantages of modern nanomedicine with compounds of natural origin that have been used in traditional medicine since ancient times. Indeed, applications of nanotechnology in the health sciences have led to the formulation of nanometric-scale systems called nanoparticle drug carriers (NPDCs) that consist of at least two components: the active principle, or biologically active molecule, and a delivery system. Compounds of this kind can perform special functions related to diagnosing, treating, and preventing certain diseases [6]. The specific properties that determine their biological impact include chemical composition, primary particle size, morphology, and solubility. These systems offer advantages like the ability to cross biological barriers to reach target organs, tissues, cell groups, or intracellular compartments, while also controlling the release of the active molecule once it reaches its action or absorption site. In these ways they contribute to resolving the challenges associated with the solubility, bioavailability, immunocompatibility and cytotoxicity of many drugs [7]. These systems can also function at the molecular level in a range of 10 - 1000 nm in at least one dimension [8].

Nanosystems made with polymers (PNPs) are solid vectors with high stability that, depending on the type of polymer used, provide such properties as controlled release, vectorization, and transport of hydrophilic and lipophilic substances that cannot otherwise cross cell membranes in living organisms [9].

Nanomedicine, in combination with traditional medicine, has allowed the development of new products, including NPDCs as vehicles for active ingredients of natural origin, such as glycyrrhizic acid (GA) [10], an antiviral compound extracted from the sweet root legume (*glycyrrhiza glabra*) that grows in subtropical regions [11] [12]. GA has therapeutic applications in various diseases of interest in both human and veterinary medicine. In this study, the *in vitro* effect of this antiviral content in poly- $\epsilon$ -caprolactone nanoparticles containing glycyrrhizic acid (PNPsGA) was evaluated as a new therapeutic strategy for treating PRRSV infections.

## 2. Materials and Methods

### 2.1. Preparation of the PNPsGA

The PNPs were prepared by the modified emulsification-diffusion method [13]. Solvent saturation was performed by mixing equal parts of water and ethyl acetate for 20 min. After separation, the two phases were recovered independently and 2 g of Mowiol 4 - 8 were dissolved in 40 ml of the aqueous phase, and 400

mg of poly- $\epsilon$ -caprolactone in 20 ml of the organic phase. Both phases were emulsified at 11,000 rpm for 10 min in Ultraturax<sup>®</sup> equipment (Cole-Parmer, USA) to form an oil-in-water emulsion (o/w). Next, 100 ml of water were added (diffusion stage) and subsequently evaporated from the solvent in a rotary evaporator for 1 h at 40°C and 60 rpm. The PNPs were left to stabilize for 24 h at 4°C, then centrifuged at 30,000 rpm for 30 min to resuspend them in 2 ml of H<sub>2</sub>O. Finally, they were added by slow flow to a 20-ml solution of acetate buffer that contained 37 mg of glycyrrhizic acid. This formulation was maintained under magnetic stirring at 500 rpm for 1 h to complete drug absorption. All reagents used were of reagent grade, obtained from Sigma-Aldrich (USA), and used with no additional purification. The water was of Milli-Q quality (Millipore<sup>®</sup>, Bedford, MD, USA).

## 2.2. Characterization

The characterization of the size, shape and stability of systems determines the properties and behavior in biological environments. Particle size by Dynamic light-scattering (DLS) was performed with a submicron laser particle counter at a scattering angle of 90° (Nanosizer<sup>®</sup> N4 Plus) and a wavelength of 680 nm for 3 min at 25°C. Samples were diluted in distilled water to within the device's sensitivity range. The scattered light data were examined using a digital correlator in the unimodal analysis mode. Only the formulations with a polydispersity index (PI) < 1 were selected. The samples were analyzed at six intervals: 1, 2, 3, 4, 15, and 30 days post-processing. After measuring them, were recovered to assess stability (zeta potential) by Doppler laser microelectrophoresis using a Zetasizer Nano HS (ZEN3600) (Malvern<sup>®</sup> Instruments Limited, UK) equipped with an He/Ne laser with a wavelength of 633 nm and 4 mW of output power. An average of 100 readings was performed. Determinations were made in triplicate for all batches prepared.

For the morphology analysis by Scanning electron microscopy (SEM) of the PNPsGA, the samples were placed in a 0.22- $\mu$ m pore filtration membrane, dried at 25°C, and placed on a grid covered with a thin gold film (~20 nm thick) for 5 min at 7 amps in a vacuum (Denton Vacuum, USA) for subsequent visualization at 25,000X using a Jeol<sup>®</sup> JSM-6010LA (USA) low vacuum, scanning electron microscope.

## 2.3. Adsorption Efficiency (EA) and Loading Capacity (LC)

The EA and LC of the GA in the PNPsGA were determined by ultracentrifugation at 20,000 rpm and 10°C for 30 min. The resulting supernatant containing glycyrrhizic acid not associated with the nanoparticles was measured by high-performance liquid chromatography (HPLC). The supernatant was then brought to a volume of 250 ml, and a 4-ml aliquot was taken and brought to a final volume of 25 ml. In the next step, 20 microliters of that solution were injected into a reverse-phase C18 column (5  $\mu$ m, 4.6 mm  $\times$  150 mm). The mobile phase was a mixture of methanol/acidified water (68.5:31.5) at 1% with glacial

acetic acid. The flow rate was 1 ml/min. The adsorption efficiency (AE%, Equation (1)) and loading capacity of the GA (LC%, Equation (2)) of the nanoparticles were calculated with the following equations:

$$AE(\%) = \frac{\text{total AG-free AG}}{\text{total AG}} \times 100 \quad (1)$$

$$LC(\%) = \frac{\text{total AG-free AG}}{\text{weight of the nanoparticles}} \times 100 \quad (2)$$

## 2.4. MARC-145 Cell Line

The MARC-145 cell line (clone of the African green monkey kidney cell line MA-104) was used in the infection challenges with PRRSV and exposure to the PNP<sub>s</sub>GA. The cells were cultured in Roswell Park Memorial Institute 1640 medium (RPMI), supplemented with 10% and 2% of fetal bovine serum (FBS) for growth and maintenance, respectively, and antibiotics (5000 IU/ml penicillin and 5 µg/ml streptomycin). The cultures were maintained in a humidified incubator with a mixture of 95:5 air/CO<sub>2</sub> at 37°C until they reached a confluence of 80% - 90%, which was considered adequate for use in the ensuing experiments.

## 2.5. Viral Spread

The VR-2332 strain of PRRSV was obtained from the commercial live virus vaccine Ingelvac<sup>®</sup> PRRS MLV at the Böhrenger Ingelheim laboratory. For propagation, MARC-145 cultures were covered with the viral solution and incubated for 2 h, then the viral solution was removed and 1 ml of RPMI medium supplemented with 2% FBS (2% RPMI) was added. The cultures were monitored every 12 hours post-infection (hpi). Upon observing cytopathic effects, they were subjected to three freezing/thawing steps to lyse the cells and release the viral load into the medium. The resulting medium was centrifuged at 5000 rpm for 20 min. The supernatant was recovered, filtered through a 0.22-µm membrane, and aliquoted under sterile conditions for later use. After propagation and recovery, the viral titers were calculated by the Reed-Muench method.

## 2.6. Viral Infection

MARC-145 cells were cultured in 24-well plates to 70% confluence. Five systems were tested:

System 1 (to determine a possible preventive effect): 50 µl/ml of PNP<sub>s</sub>GA were added to each well. After 4 h, the cultures were washed with sterile 3% RPMI and infected for 1 h with 200 µl of PRRSV, then the virus was removed and 3% RPMI medium was added to monitor the course of the infection.

System 2 (to determine a possible inhibitory effect): cell cultures with 70% confluence were infected for 1 h with 200 µl of PRRSV. When the viral solution was added, 50 µl/well of PNP<sub>s</sub>GA were administered, then the virus and PNP solution were removed and 3% RPMI medium was added to monitor the course of the infection.

System 3 (to determine a possible therapeutic effect): after viral infection and

the addition of RPMI 3% medium, 50  $\mu$ l/well of the PNP<sub>s</sub>GA were added to monitor the course of the infection.

System 4 (control of viral infection): cultures were infected for 1 h with 200  $\mu$ l of PRRSV, then the virus was removed and 3% RPMI medium was added to monitor the course of the infection.

System 5 (uninfected culture): once confluence was reached, the 3% RPMI medium was changed to continue with the culture.

All systems were maintained for 96 hpi and evaluated at 4 intervals (24, 48, 72, 96 hpi).

## 2.7. Hematoxylin and Eosin Staining

After exposure to the different systems, cells seeded on circular slides were fixed with a 4% paraformaldehyde solution for 10 min, washed with phosphate buffered saline (PBS), and covered with a 1% hematoxylin solution for 20 min. At that point, washes were carried out with PBS and the cells were covered for 10 min with eosin. Finally, they were washed with PBS and mounted on slides with resin.

## 2.8. Cell Viability

For the MTT (3-(4,5-dimethylthiazol-2-yl)-2,5-diphenyl tetrazolium bromide) assay [14], the culture medium was added to a 0.5 mg/ml MTT solution and incubated for 3 h in a humidified environment with 5% CO<sub>2</sub> at 37°C. Subsequently, 330  $\mu$ l of dimethyl sulfoxide (DMSO) were added and product intensity was analyzed by spectrophotometry at 570 nm in a plate reader (enzyme-linked immunosorbent assay, ELISA).

## 2.9. Cell Viability by Exclusion of Trypan Blue

These samples were incubated at a 1:1 ratio of 0.4% (w/v) trypan blue solution for 10 min using automated equipment (TC20™ Automated Cell Counter, Bio-Rad, USA) in a detection concentration range of  $5 \times 10^4$  -  $1 \times 10^7$  cells/ml. Next, 10  $\mu$ l of the cell suspension were placed in duplicate on a slide with a double counting chamber (C20™ counting slides, Bio-Rad, USA), and introduced immediately into the equipment for counting.

## 2.10. RT-qPCR

For the real-time quantitative polymerase chain reaction (RT-qPCR) technique, the POCKIT™ PRRSV-NA reagent set (GeneReach Biotech, Taichung, Taiwan) was used to detect two of the best conserved regions of the ORF6 and ORF7 genes in the PRRSV genome. Samples were processed using the TRIzol® method (Reagent Total RNA Isolation Reagent, Life Technologies). The primers used to identify ORF5-7 were forward 5'-*TTT GGC AAT GTG TCA GGC ATC GTG-3'* and reverse 5'-*CCA TTC ACC ACA CAT TCT TCC-3'*.

## 2.11. Statistical Analysis

The data obtained were analyzed independently using a completely randomized

design. The separation of means was performed using a Tukey's test. The data were subjected to an analysis of variance (ANOVA) using the GraphPad Prism 7 package with a significance level of  $\alpha = 0.05$  to detect between-group differences. ImageJ software was used for image analysis.

### 3. Results

The PNP<sub>s</sub>GA were elaborated following the reference in Jardon *et al.*, (2018) [15]. Subsequent measurement by the DLS technique determined that the PNP<sub>s</sub>GA had a nanometric size with a maximum intensity peak at  $217.43 \pm 11.44$  nm, and a polydispersity index of  $0.17 \pm 0.04$ , which is indicative of a homogeneous size distribution. During the evaluation period, the partial particle size of each system was measured weekly to evaluate the physical stability of the formulations, which remained on a nanometric scale for up to 6 months at room temperature without light protection. To validate the data obtained from the partial particle size study using the DLS technique, the samples were observed under scanning electron microscopy. Measurements of the nanometric size obtained by DLS were consistent with those of the micrographs, which not only showed structures <1 micrometer but also allowed us to determine that each system had a spherical morphology that tended to agglomerate during drying and then form films (Figure 1).

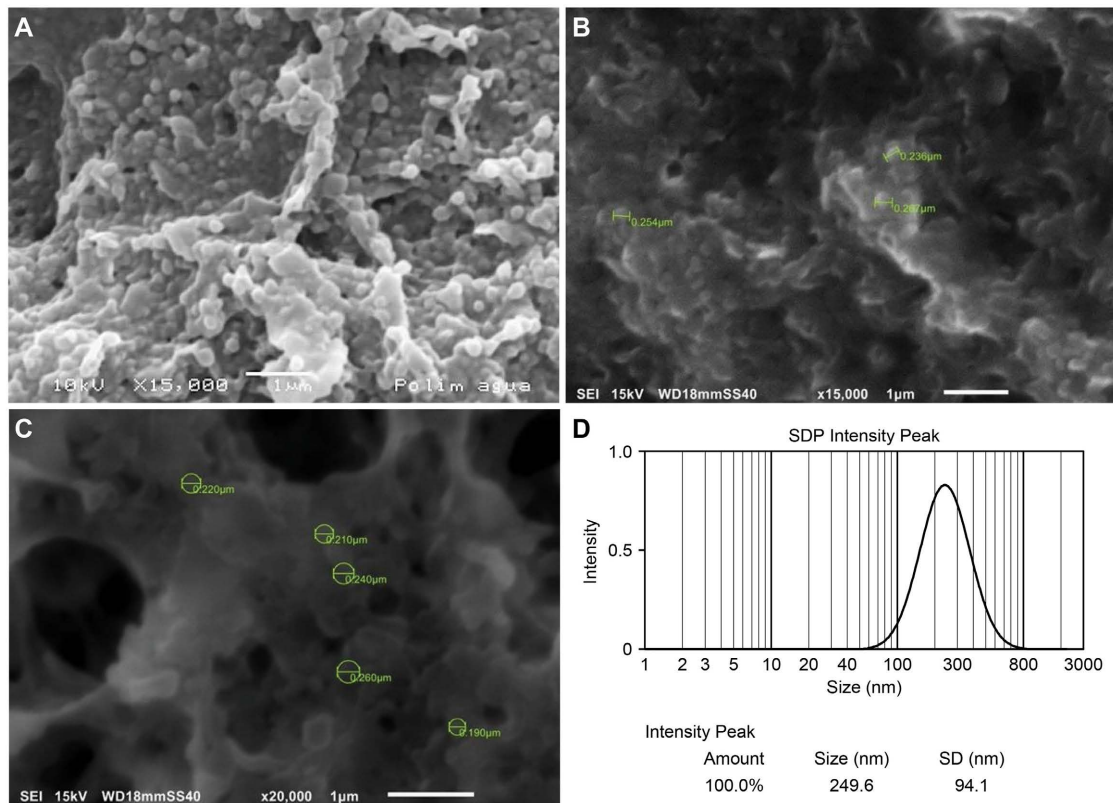


**Figure 1.** Scanning electron microscopy of PNP<sub>s</sub>. Images were taken with SEM at 15,000X (A, B) and 20,000X (C). Micrographs show that the nanotransporters have a size < 1 micrometer and spherical shapes. Bar = 1 μm. PNP intensity peak graph (D).



After obtaining and characterizing the systems, the PNP<sub>s</sub>GA were sterilized with UV light to assess their antiviral effect on MARC-145 cultures infected with PRRSV. The size of the PNP<sub>s</sub>GA was determined before and after exposure to UV light to verify that nanometric size was maintained. During preparation of the lots of PNP<sub>s</sub>GA, the load capacity of the samples for GA was evaluated, determining a capacity of  $58.81 \pm 0.14$ .

All tests of the cell cultures were performed using MARC-145 cells, as this infection model is useful in research into the action mechanisms of this virus and the effectiveness of new antiviral systems [15].

The cytopathic effect produced by infection with PRRSV was visible when the cultures were evaluated by bright field microscopy. This effect was characterized by the acquisition of a rounded shape, loss of the nucleus-cytoplasm relation, vacuolization, formation of syncytia, and cell lysis (Figure 2). Results showed that PRRSV had a severe cytopathic effect after 48 hpi, as it destroyed 76.8% of the monolayer. To evaluate the effects on morphology during acute infection, the cultures were stained with hematoxylin and eosin (H&E), which showed changes after 24 hpi (Figure 3) that included lysis, vacuolization, and the formation of syncytia (Figure 3B).

The most pronounced cytopathic effect occurred in the range of 48-72 hpi, where the damage to the integrity of the monolayer was >70% (Figure 2). The adhered cells presented an isolated distribution with numerous vacuoles at the cytoplasmic level that produced a granular aspect, loss of the nucleus-cytoplasm relation, and morphological changes ranging from rounded forms (Figure 3D) to a fusiform shape with pyknotic nuclei (Figure 3E) that ended with the detachment of the monolayer due to cell lysis (Figure 3F).

Based on the cytopathic effects induced by *in vitro* infection with PRRSV, 48 and 72 hpi were chosen to evaluate cell viability by the MTT assay (Figure 4) and exclusion with trypan blue (Figure 5). Pretreatment with 50  $\mu$ l of PNPs for 4 h decreased the cytotoxicity determined by the MTT assay by 38% compared to untreated infected cells, while the behavior of cell viability measured by the trypan blue test was 22%.

The effect of the PNP<sub>s</sub>GA on viral replication was evaluated by reverse transcription, followed by real-time quantitative PCR (RT-qPCR) analysis of the PRRSV RNA level. As Figure 6 shows, treatment with the PNP<sub>s</sub>GA reduced the number of RNA copies of PRRSV in 3 cycles.

#### 4. Discussion

This study analyzed the antiviral potential of a model of nanoparticles with glycyrrhizic acid (Figure 1), a component of natural origin that has been shown to have an antiviral effect [11] [16] [17]. On viruses such as influenza A [18], (Harada 2005), herpes simplex virus type 1 (HSV-1), human papillomavirus [19] and Newcastle virus [16] [20] [21] [22]. It also decreases the replication of viruses like severe acute respiratory syndrome (SARS) [23]. Glycyrrhizic acid contained in carbon dots has been reported to suppress the spread of pseudorabies

virus (PRV) and porcine epidemic diarrhea virus (PEDV), suggesting the broad antiviral activity in pigs [24] [25]. However, GA has certain drawbacks; namely, poor solubility in water, and some degree of cytotoxicity [26]. For this reason, it is necessary to use nanotransporters; that is, systems designed to improve the pharmacokinetics of antivirals because their nanometric size confers important characteristics, including the ability to cross biological barriers and avoid the premature degradation of active agents, among others [6]. The nature of the materials used to make them gives unique properties. Polymeric NPs have a limited loading capacity, but the nature of their components means they are considered biodegradable with low toxicity and good tolerance in biological systems [10] [15] [27] [28] [29].

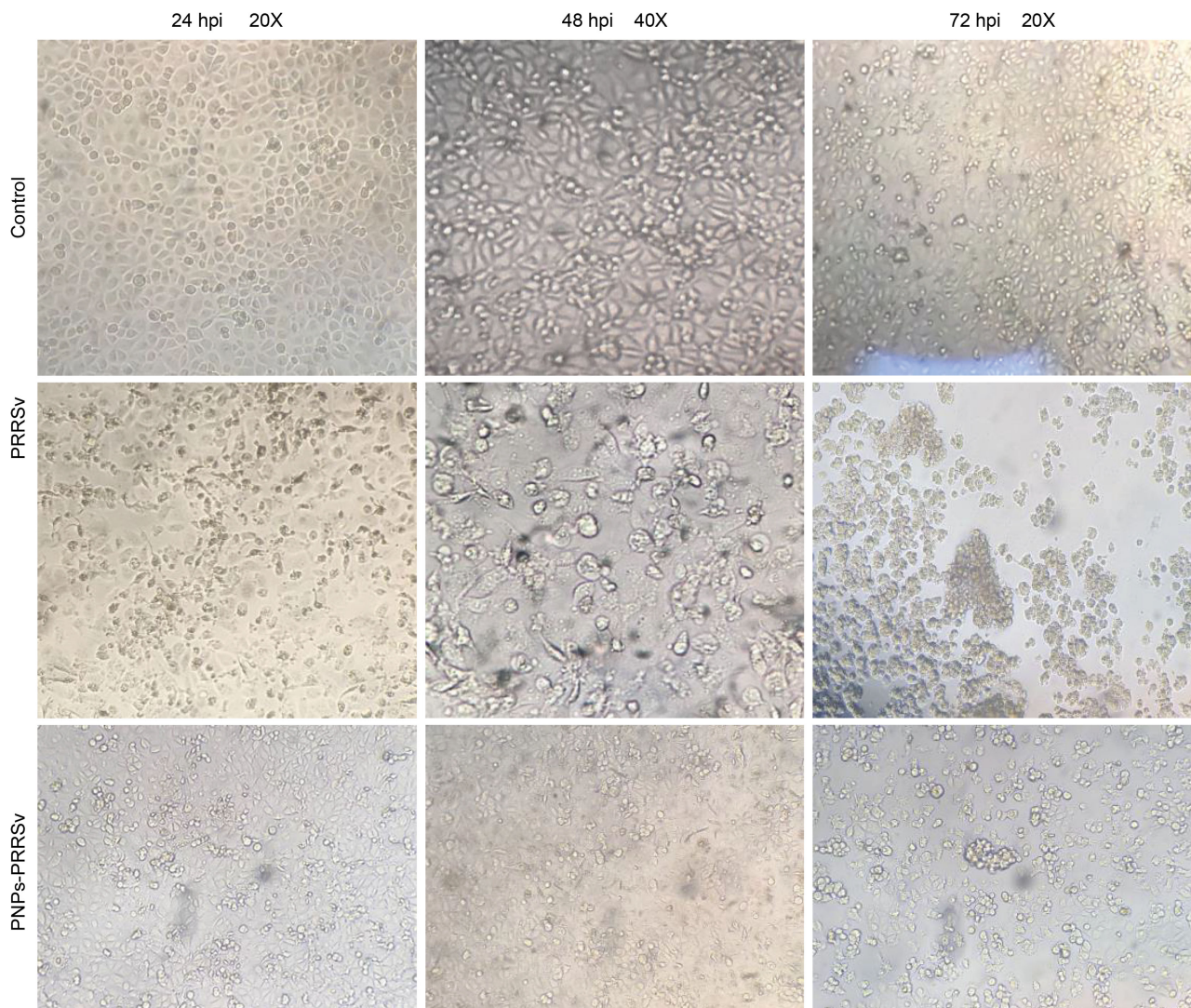


**Figure 2.** Effect of PNP pretreatment on MARC-145 cell cultures. PRRSV-induced cytopathic changes in MARC-145 cells. Foci of damage were observed during the period from 24 - 72 hpi. Top row: MARC-145 control cultures. Middle row: MARC-145 cell culture infected with PRRSV. Bottom row: MARC-145 culture cells treated with PNPs 4 h prior to PRRSV infection. Cytopathic damage in the cultures decreased during PRRSV infection with PNP pretreatment 4 hours prior to MARC-145 infection. Clear field microscopy at 20X and 40X. Images obtained from 3 independent experiments.



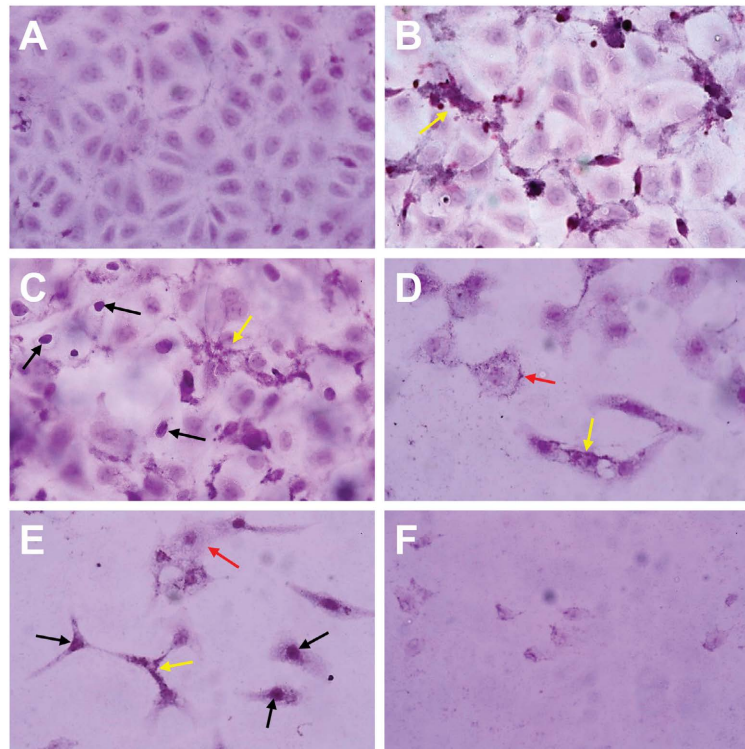


**Figure 3.** Morphological evaluation of MARC-145 cells infected in vitro with PRRSV. (A) control, (B) 24 hpi, (C) 48 hpi, (D, E) 72 hpi, (F) 96 hpi with H&E staining. Black arrows indicate the presence of pycnotic nuclei. Yellow arrows indicate the presence of r-type basophilic material at the cytoplasmic level. Red arrows indicate vacuolization zones.

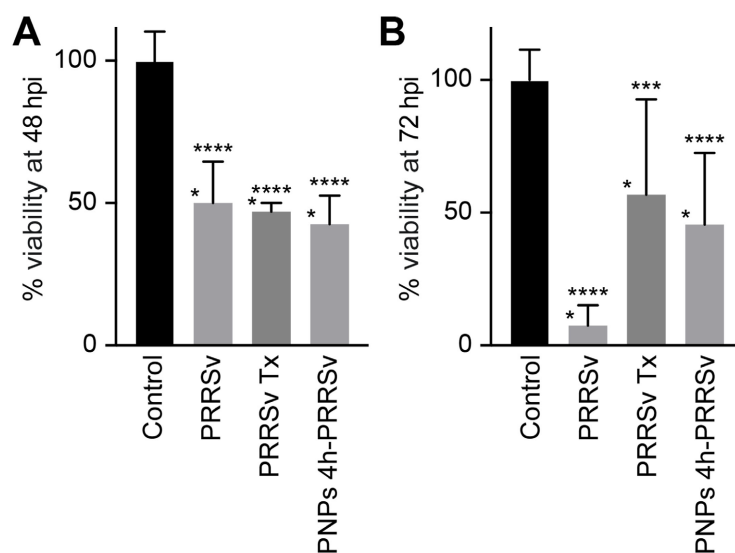


**Figure 4.** Assessment of viability in cultures of MARC-145 cells treated with GA (A). Data from PNP treatments at 48 hpi showed no significant difference between cultures infected with PRRSV and those infected with the virus incubated 12 h prior to infection with PNPsGA (PRRSv Tx) and those treated with PNPs 4 h pre-infection (PNPs 4 h-PRRSv). However, at 72 hpi, a protective effect was observed with a significant difference (B). ANOVA, \*\*\* $P < 0.001$ , \*\* $P < 0.01$ , and \* $P < 0.05$ . Data obtained from 3 independent experiments by MTT.

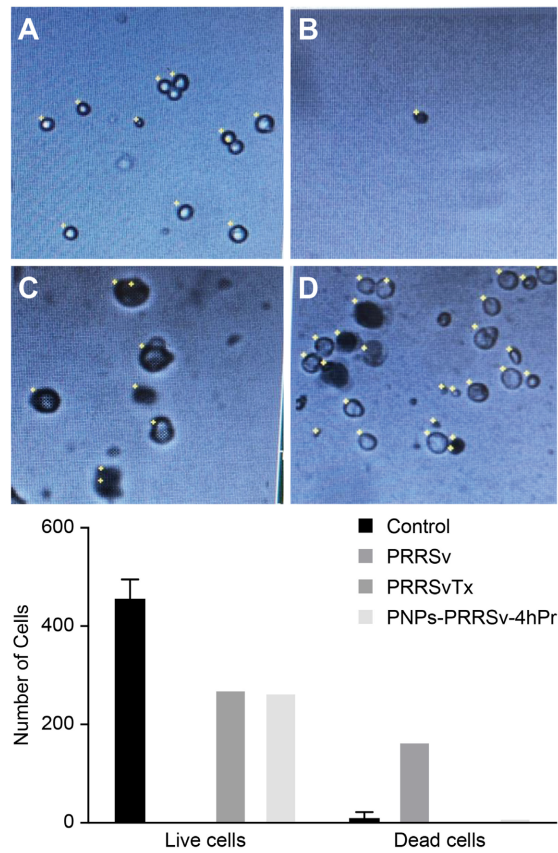


**Figure 5.** Trypan blue exclusion. The effect of PNPsGA treatment on cell viability in PRRSV-infected cultures at 72 hpi was also demonstrated by trypan blue staining. (A) Refringent cells that correspond to viable cells in the control culture; and (B) cell stained with dye in an PRRSV-infected culture, revealed as a dead cell. Culture cells treated with PNPsGA 4 h pre-infection with PRRSV, viable (refringent) and dead (blue) cells at 48 hpi (C) and 72 hpi (D). Figure (D) shows an increase in cell number and viability.

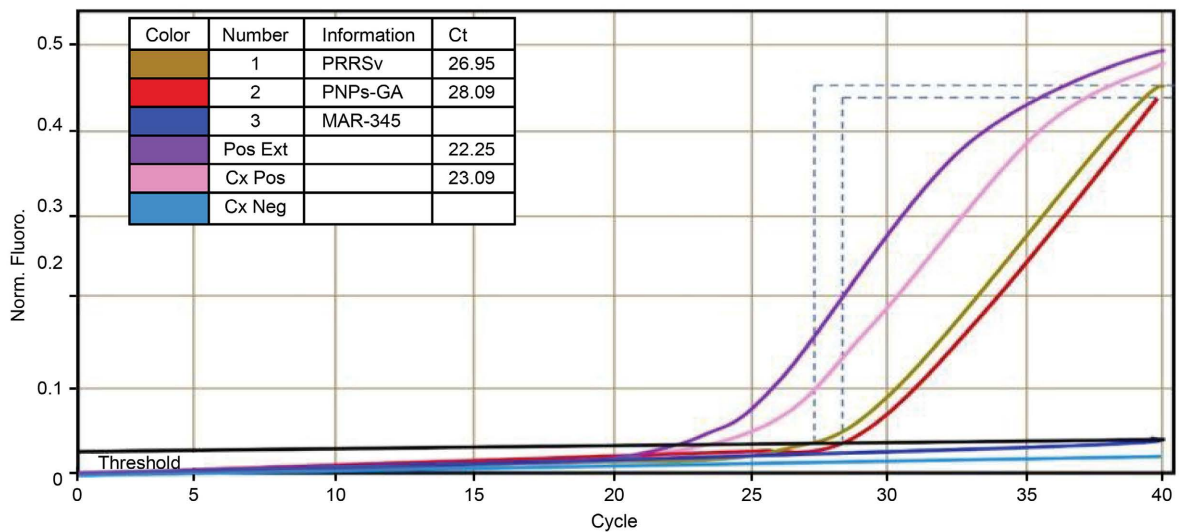


**Figure 6.** RT-qPCR vs. PRRSV curves. Quantification data and amplification curves for PRRSV-infected crops (red) and cultures treated with PNPs (olive green). Treatment with PNPs decreased the amplification and detection of PRRSV sequences by RT-PCR by 2 - 3 cycles (bridged green line vs. dotted red line (PRRSv)).

Viral agents represent a significant challenge for human and animal health. One of the diseases recognized as having the greatest negative economic impact on the global swine industry is porcine respiratory and reproductive syndrome [1] [30] [31] [32]. In their studies of this disease, Kim (1993) [33] and Dea (1995) [34] reported that the MARC-145 cell line is highly permissive for replicating PRRSV. Based on those reports, MARC-145 cultures have emerged as the primary choice for replicating this pathogen. In the present study, 4 intervals (24 - 96 hpi) were tested to evaluate the cytopathic changes induced by PRRSV and the effects of PNP<sub>s</sub>GA pre- and post-infection and at coinfection [35] [36]. Some authors have reported that the cytopathic effects in porcine alveolar macrophages occur at 16 hpi and end at 24 hpi with total cell destruction. This effect occurs later in MARC-145 cultures, where cytopathic effects are reported at 48 h, a time similar to the changes observed in this study, followed by a predominant period of damage from 48 - 72 hpi, with the maximum peak of affectation occurring at 72 h [37] [38], (Zhang 2011; Howerth 2002), concluding with the detachment of the monolayer at 96 hpi [39].

In the viral infection assays, coadministration (PNP<sub>s</sub>GA + PRRSV) and 12 hpi treatment (PNP<sub>s</sub>GA and PRRSV administered at 12 hpi) showed no significant differences in the infected cultures (PRRSV), thus ruling out a possible inhibitory and/or therapeutic effect. The course of infection was similar to that in the positive control (PRRSV) in that it ended with the destruction of the monolayer, a result similar to that obtained by Duan *et al.*, (2015) [40], who reported no evidence of effects on viral penetration and absorption capacity in MARC-145 cells when the virus was treated with GA. Their results may be related to reports that GA mainly inhibits the viral penetration but has little effect on the absorption or release phases of PRRSV infection during its life-cycle [40] [41].

The presence of direct inhibitory action of PNP<sub>s</sub>GA on the PRRSV viral particles was thus excluded. In addition, incubation of PRRSV with PNP<sub>s</sub>GA for 24 h to evaluate a possible inhibitory effect on the infective capacity of the particles led to this being ruled out, as well, because effects similar to those on the infected cells were observed with PRRSV. These findings highlight the fact that GA inhibits the proliferation of PRRSV mainly during the internalization stage of the virus, but has no apparent effect on the direct inactivation of PRRSV particles. In 2015, Duan [40] similarly reported that coincubation of PRRSV with GA at concentrations of 20, 40, and 80  $\mu$ M had no effect on the ability of PRRSV to infect MARC-145 cells, thus demonstrating that GA does not directly inactivate PRRSV particles.

The effects reported in earlier assays are attributable to active infection by PRRSV, so the RT-qPCR test showed the presence of the virus in cultures infected with PRRSV, without a positive signal in the control cultures (Figure 6). This led to the determination that the cytopathic changes observed are attributable to the process of viral infection. The greatest antiviral effect of PNP<sub>s</sub>GA was observed in MARC-145 cells pretreated for 4 h. These results can be explained by the recognized capacity of nanotransporters to act as structures that improve the cell pene-

tration capacity of certain drugs. This effect is observed even with the concentration of the active principle in PNPsgA. In cultures treated 4 h pre-infection with PRRSV (Figure 6, olive green line), the number of cycles necessary for the threshold cycle (TC) was slightly higher than in the ones infected with PNPsgA without pretreatment (Figure 6, red line). This suggests the need for assays carried out at distinct concentrations of PNPsgA and pre-infection times.

An active ingredient in herbal medicine, glycyrrhizic acid has played an important role as an antioxidant, anti-inflammatory, antiviral immunoregulator, and liver protector [22] [42]; as recent research shows [41]. However, it presents problems of solubility, cytotoxicity, degradation, and biocompatibility, so the nontoxic metabolism of polymer nanomaterials is an alternative for transporting this type of drug. The antiviral mechanism of PNPsgA was demonstrated by the inhibition of invasion and *in vitro* replication of PRRSV, which showed that this formulation has good antiviral activity against PRRSV ( $\approx 3$  orders of magnitude) and increases cell viability by 38% for up to 72 h.

## 5. Conclusion

In this study, the antiviral effect of a PNPsgA was evaluated, determining that this a stable system has glycyrrhizic acid loading capacity, which inhibits the invasion and replication of PRRSV as its the most important mechanism, was developed and evaluated. It reduced cellular damage induced by PRRSV infection by 38% in MARC cells, with a decrease of 3 amplification cycles and detection of PRRSV sequences by RT-qPCR when administered in cell cultures 4 h preinfection. The development of this technology could suggest a preventive therapeutic effect. However, additional studies of the effect of the viral penetration process are needed, the formulation needs to be optimized to increase its capacity to transport GA and evaluate the therapeutic potential associated with the concentration of the active ingredient. Finally, our cellular model of infection is a useful tool for conducting research on the action mechanisms of this virus, and evaluating the effectiveness of new nanoparticle systems for the transport of antiviral substances that provide a more effective way to deal with PRRSV.

## Ethics Statement

The authors confirm that the ethical policies of the journal, as noted on the author guidelines page, have been adhered to. No ethical approval was required as the work conducted is original research on cell cultures.

## Conflicts of Interest

The authors declare no conflicts of interest regarding the publication of this paper.

## References

- [1] Zimmerman, J., Benfield, D.A., Murtaugh, M.P., Osorio, F., Stevenson, G.W. and

- Torremorell, M. (2006) Porcine Reproductive and Respiratory Syndrome Virus (Porcine Arterivirus). *Diseases of Swine*, **9**, 387-418.
- [2] Lunney, J.K., Benfield, D.A. and Rowland, R.R. (2010) Porcine Reproductive and Respiratory Syndrome Virus: An Update on an Emerging and Re-Emerging Viral Disease of Swine. *Virus Research*, **154**, 1-6.  
<https://doi.org/10.1016/j.virusres.2010.10.009>
- [3] Dénes, L., Horváth, D.G., Duran, O., Ratkhjen, P.H., Kraft, C., Acs, B., Szász, A.M., Rűmenapf, T., Papp, M., Ladinig, A. and Balka, G. (2021) *In situ* Hybridization of PRRSV-1 Combined with Digital Image Analysis in Lung Tissues of Pigs Challenged with PRRSV-1. *Veterinary Sciences*, **8**, Article 235.  
<https://doi.org/10.3390/vetsci8100235>
- [4] Lyoo, K.S., Yeom, M., Choi, J.Y., Park, J.H., Yoon, S.W. and Song, D. (2015) Unusual Severe Cases of Type 1 Porcine Reproductive and Respiratory Syndrome Virus (PRRSV) Infection in Conventionally Reared Pigs in South Korea. *BMC Veterinary Research*, **11**, Article No. 272.  
<https://bmcvetres.biomedcentral.com/articles/10.1186/s12917-015-0584-5>  
<https://doi.org/10.1186/s12917-015-0584-5>
- [5] Huang, Y.W. and Meng, X.J. (2010) Novel Strategies and Approaches to Develop the Next Generation of Vaccines against Porcine Reproductive and Respiratory Syndrome Virus (PRRSV). *Virus Research*, **154**, 141-149.  
<https://doi.org/10.1016/j.virusres.2010.07.020>
- [6] Irache, J.M. (2008) Nanomedicina: Nanopartículas con aplicaciones médicas. *Anales del Sistema Sanitario de Navarra*, **31**, 7-10.  
[https://scielo.isciii.es/scielo.php?script=sci\\_arttext&pid=S1137-66272008000100001](https://scielo.isciii.es/scielo.php?script=sci_arttext&pid=S1137-66272008000100001)  
<https://doi.org/10.4321/S1137-66272008000100001>
- [7] Jabr-Milane, L., Van Vlerken, L., Devalapally, H., Shenoy, D., Komareddy, S., Bhavsar, M. and Amiji, M. (2008) Multi-Functional Nanocarriers for Targeted Delivery of Drugs and Genes. *Journal of Controlled Release*, **130**, 121-128.  
<https://doi.org/10.1016/j.jconrel.2008.04.016>
- [8] Tsuji, J.S., Maynard, A.D., Howard, P.C., James, J.T., Lam, C.W., Warheit, D.B. and Santamaria, A.B. (2006) Research Strategies for Safety Evaluation of Nanomaterials, Part IV: Risk Assessment of Nanoparticles. *Toxicological Sciences*, **89**, 42-50.  
<https://doi.org/10.1093/toxsci/kfi339>
- [9] Escalona, R.O. and Quintanar, G.D. (2014) Nanogeles poliméricos: Una nueva alternativa para la administración de fármacos. *Revista mexicana de ciencias farmacéuticas*, **45**, 17-38. <https://www.redalyc.org/articulo.oa?id=57935447003>
- [10] Urbán, M.Z. (2015) Evaluación de la actividad terapéutica del ácido glicirricínico formulado en sistemas submicrónicos contra el virus de PRRS. Master's Thesis, Universidad Nacional Autónoma de México, Mexico City.  
[https://repositorio.unam.mx/contenidos/evaluacion-de-la-actividad-terapeutica-del-acido-glicirricinico-formulado-en-sistemas-submicronicos-contra-el-viru-78492?c=4A07aE&d=true&q=\\*&i=4&v=1&t=search\\_0&as=0](https://repositorio.unam.mx/contenidos/evaluacion-de-la-actividad-terapeutica-del-acido-glicirricinico-formulado-en-sistemas-submicronicos-contra-el-viru-78492?c=4A07aE&d=true&q=*&i=4&v=1&t=search_0&as=0)
- [11] Aguilar, R.I., Alcalá, A.S., Llera, R.V. and Ganem, R.A. (2015) Preparation and Characterization of Mucoadhesive Nanoparticles of Poly (Methyl Vinyl Ether-Co-Maleic Anhydride) Containing Glycyrrhizic Acid Intended for Vaginal Administration. *Drug Development and Industrial Pharmacy*, **41**, 1632-1639.  
<https://doi.org/10.3109/03639045.2014.980425>
- [12] Izutani, Y., Kanaori, K. and Oda, M. (2014) Aggregation Property of Glycyrrhizic Acid and Its Interaction with Cyclodextrins Analyzed by Dynamic Light Scattering, Isothermal Titration Calorimetry, and NMR. *Carbohydrate Research*, **392**, 25-30.



- <https://doi.org/10.1016/j.carres.2014.04.017>
- [13] Jardon, X.S. (2020) Estudio del efecto biológico en líneas celulares de nanopartículas lipídicas y poliméricas como vehículo de ácido glicirricínico para el tratamiento del virus de PRRS. Master's Thesis, Universidad Nacional Autónoma de México, México City. <http://132.248.9.195/ptd2020/enero/0799986/Index.html>
- [14] Mosmann, T. (1983) Rapid Colorimetric Assay for Cellular Growth and Survival: Application to Proliferation and Cytotoxicity Assays. *Journal of Immunological Methods*, **65**, 55-63. [https://doi.org/10.1016/0022-1759\(83\)90303-4](https://doi.org/10.1016/0022-1759(83)90303-4)
- [15] Jardon-Xicotencatl, S., García-Tovar, C.G., Quintanar-Guerrero, D., Nieto-Bordes, J.L. and Juárez-Mosqueda, M.L. (2018) Effect of Two Glycyrrhizic Acid Nanoparticle Carriers on MARC-145 Cells Actin Filaments. *Applied Nanoscience*, **8**, 1111-1121. <https://doi.org/10.1007/s13204-018-0758-0>
- [16] Baltina, L.A., Kondratenko, R.M., Plyasunova, O.A., Pokrovskii, A.G. and Tolstikov, G.A. (2009) Prospects for the Creation of New Antiviral Drugs Based on Glycyrrhizic Acid and Its Derivatives (A Review). *Pharmaceutical Chemistry Journal*, **43**, 539-548. <https://doi.org/10.1007/s11094-010-0348-2>
- [17] Baltina, L.A., Kondratenko, R.M., Baschenko, N.Z. and Pl'yasunova, O.A. (2015) Synthesis and Biological Activity of New Glycyrrhizic Acid Conjugates with Amino Acids and Dipeptides. *Russian Journal of Bioorganic Chemistry*, **35**, 510-517. <https://doi.org/10.1134/S1068162009040141>
- [18] Harada, S. (2005) The Broad Anti-Viral Agent Glycyrrhizin Directly Modulates the Fluidity of Plasma Membrane and HIV-1 Envelope. *Biochemical Journal*, **392**, 191-199. <https://doi.org/10.1042/BJ20051069>
- [19] Cáceres, S.O., Fragoso, R.R., Mena, C.C., et al. (2015) Hiperplasia Multiepitelial Focal: Tratamiento Comparativo, Ácido Glicirricínico Contra Nitrógeno Líquido. *Revista Odontológica Mexican*, **19**, 101-105. [https://www.scielo.org.mx/scielo.php?script=sci\\_arttext&pid=S1870-199X2015000200006](https://www.scielo.org.mx/scielo.php?script=sci_arttext&pid=S1870-199X2015000200006)  
<https://doi.org/10.1016/j.rodex.2015.05.007>
- [20] Pompei, R., Flore, O., Marccialis, M.A., Pani, A. and Loddo, B. (1979) Glycyrrhizic Acid Inhibits Virus Growth and Inactivates Virus Particles. *Nature*, **281**, 689-690. <https://doi.org/10.1038/281689a0>
- [21] Pompei, R., Paghi, L., Ingianni, A. and Ucheddu, P. (1983) Glycyrrhizic Acid Inhibits Influenza Virus Growth in Embryonated Eggs. *Microbiologica*, **6**, 247-250. <https://pubmed.ncbi.nlm.nih.gov/6633273/>
- [22] Pompei, R., Pani, A., Flore, O., Marccialis, M.A. and Loddo, B. (1980) Antiviral Activity of Glycyrrhizic Acid. *Cellular and Molecular Life Sciences*, **36**, 304. <https://doi.org/10.1007/BF01952290>
- [23] Cinatl, J., Morgenstern, B., Bauer, G., Chandra, P., Rabenau, H. and Doerr, H.W. (2003) Glycyrrhizin, an Active Component of Licorice Roots, and Replication of SARS-Associated Coronavirus. *The Lancet*, **361**, 2045-2046. [https://doi.org/10.1016/S0140-6736\(03\)13615-X](https://doi.org/10.1016/S0140-6736(03)13615-X)
- [24] Wong, G., Lu, J., Zhang, W. and Gao, G.F. (2019) Pseudorabies Virus: A Neglected Zoonotic Pathogen in Humans? *Emerging Microbes & Infections*, **8**, 150-154. <https://doi.org/10.1080/22221751.2018.1563459>
- [25] Lee, C. (2015) Porcine Epidemic Diarrhea Virus: An Emerging and Re-Emerging Epizootic Swine Virus. *Virology Journal*, **12**, Article No. 193. <https://doi.org/10.1186/s12985-015-0421-2>
- [26] Størmer, F.C., Reistad, R. and Alexander, J. (1993) Glycyrrhizic Acid in Liquo-

- rice—Evaluation of Health Hazard. *Food and Chemical Toxicology*, **31**, 303-312. [https://doi.org/10.1016/0278-6915\(93\)90080-I](https://doi.org/10.1016/0278-6915(93)90080-I)
- [27] Escalona, R.O. (2017) Desarrollo y caracterización de nanopartículas con superficie modificada como potenciales transportadores de fármacos a través de la barrera hematoencefálica. Tesis Maestría, Programa de Maestría y Doctorado en Ciencias Químicas. Universidad Nacional Autónoma de México. [https://repositorio.unam.mx/contenidos/desarrollo-y-caracterizacion-de-nanoparticulas-con-superficie-modificada-como-potenciales-transportadores-de-far-293362?c=B7Zq0A&d=false&q=\\*&i=1&v=1&t=search\\_0&as=0](https://repositorio.unam.mx/contenidos/desarrollo-y-caracterizacion-de-nanoparticulas-con-superficie-modificada-como-potenciales-transportadores-de-far-293362?c=B7Zq0A&d=false&q=*&i=1&v=1&t=search_0&as=0)
- [28] Garzón, M.L., Hernández, A., Vázquez, M.L., Villafuerte, L. and García, B. (2008) Preparación de nanopartículas sólidas lipídicas (SLN), y de Acarreadores lipídicos nanoestructurados (NLC). *Revista Mexicana de Ciencias Farmacéuticas*, **39**, 50-66. <https://www.redalyc.org/articulo.oa?id=57911113008>
- [29] Quintanar, G.D., Tamayo, E.D., Ganem, Q.A., Allémann, E. and Doelker, E. (2005) Adaptation and Optimization of the Emulsification-Diffusion Technique to Prepare Lipidic Nanospheres. *European Journal of Pharmaceutical Sciences*, **26**, 211-218. <https://doi.org/10.1016/j.ejps.2005.06.001>
- [30] Albina, E. (1997) Epidemiology of Porcine Reproductive and Respiratory Syndrome (PRRS): An Overview. *Veterinary Microbiology*, **55**, 309-316. [https://doi.org/10.1016/S0378-1135\(96\)01322-3](https://doi.org/10.1016/S0378-1135(96)01322-3)
- [31] Tian, K., Yu, X., Zhao, T., Feng, Y., Cao, Z., Wang, C. and Liu, D. (2007) Emergence of Fatal PRRSV Variants: Unparalleled Outbreaks of Atypical PRRS in China and Molecular Dissection of the Unique Hallmark. *PLOS ONE*, **2**, e526. <https://www.ncbi.nlm.nih.gov/pmc/articles/PMC1885284/> <https://doi.org/10.1371/journal.pone.0000526>
- [32] Dea, S., Gagnon, C.A., Mardassi, H., Pirzadeh, B. and Rogan, D. (2000) Current Knowledge on the Structural Proteins of Porcine Reproductive and Respiratory Syndrome (PRRS) Virus: Comparison of the North American and European Isolates. *Archives of Virology*, **145**, 659-688. <https://doi.org/10.1007/s007050050662>
- [33] Kim, H.S., Kwang, J., Yoon, I.J., Joo, H.S. and Frey, M.L. (1993) Enhanced Replication of Porcine Reproductive and Respiratory Syndrome (PRRS) Virus in a Homogeneous Subpopulation of MA-104 Cell Line. *Archives of Virology*, **133**, 477-483. <https://doi.org/10.1007/BF01313785>
- [34] Dea, S., Sawyer, N., Alain, R. and Athanassious, R. (1995) Ultrastructural Characteristics and Morphogenesis of Porcine Reproductive and Respiratory Syndrome Virus Propagated in the Highly Permissive MARC-145 Cell Clone. In: Talbot, P.J. and Levy, G.A., Eds., *Corona- and Related Viruses*, Springer, Boston, 95-98. [https://doi.org/10.1007/978-1-4615-1899-0\\_13](https://doi.org/10.1007/978-1-4615-1899-0_13)
- [35] Flores-Mendoza, L., Silva-Campa, E., Reséndiz, M., Mata-Haro, V., Osorio, F.A. and Hernández, J. (2009) Efecto del virus del síndrome reproductivo y respiratorio porcino (PRRS) en células dendríticas de cerdo derivadas de monocitos. *Veterinaria México*, **40**, 39-54. [https://www.scielo.org.mx/scielo.php?script=sci\\_arttext&pid=S0301-50922009000100005](https://www.scielo.org.mx/scielo.php?script=sci_arttext&pid=S0301-50922009000100005)
- [36] Du, Y., Yoo, D., Paradis, M.A. and Scherba, G. (2011) Antiviral Activity of Tilmicosin for Type 1 and Type 2 Porcine Reproductive and Respiratory Syndrome Virus in Cultured Porcine Alveolar Macrophages. *Journal of Antivirals & Antiretrovirals*, **3**, 28-33. <https://www.longdom.org/open-access/antiviral-activity-of-tilmicosin-for-type-1-and-type-2-porcine-reproductive-and-respiratory-syndrome-virus-in-cultured-p-585>

- [7.html](#)  
<https://doi.org/10.4172/jaa.1000031>
- [37] Zhang, S., Zhou, Y., Jiang, Y., Li, G., Yan, L., Yu, H. and Tong, G. (2011) Generation of an Infectious Clone of HuN4-F112, an Attenuated Live Vaccine Strain of Porcine Reproductive and Respiratory Syndrome Virus. *Virology Journal*, **8**, Article No. 410. <https://doi.org/10.1186/1743-422X-8-410>
- [38] Howerth, E.W., Murphy, M.D. and Roberts, A.W. (2002) Failure of Porcine Reproductive and Respiratory Syndrome Virus to Replicate in Porcine Endothelial Cell Cultures. *Journal of Veterinary Diagnostic Investigation*, **14**, 73-76. <https://doi.org/10.1177/104063870201400117>
- [39] Zhang, O. and Yoo, D. (2015) PRRS Virus Receptors and Their Role for Pathogenesis. *Veterinary Microbiology*, **177**, 229-241. <https://doi.org/10.1016/j.vetmic.2015.04.002>
- [40] Duan, E., Wang, D., Fang, L., Ma, J., Luo, J., Chen, H. and Xiao, S. (2015) Suppression of Porcine Reproductive and Respiratory Syndrome Virus Proliferation by Glycyrrhizin. *Antiviral Research*, **120**, 122-125. <https://doi.org/10.1016/j.antiviral.2015.06.001>
- [41] Tong, T., Hu, H., Zhou, J., Deng, S., Zhang, X., Tang, W. and Liang, J. (2020) Glycyrrhizic-Acid-Based Carbon Dots with High Antiviral Activity by Multisite Inhibition Mechanisms. *Small*, **16**, Article ID: 1906206. <https://doi.org/10.1002/sml.201906206>
- [42] Zhang, Q. and Ye, M. (2009) Chemical Analysis of the Chinese Herbal Medicine Gan-Cao (Licorice). *Journal of Chromatography A*, **1216**, 1954-1969. <https://doi.org/10.1016/j.chroma.2008.07.072>